Instantaneous phase and the detection of lateral wavelet stability

MIKE PERZ, *Geo-X Systems Ltd., Calgary, Canada*
MAURICIO D. SACCHI, *University of Alberta, Edmonton, Canada*
ANN O'BYRNE, *EnCana Corporation, Calgary, Canada*

When it comes to the evaluation of stratigraphic plays, the issue of lateral wavelet stability ranks as an important concern. Interpreters accustomed to working complex structural plays may be inclined to relegate this type of concern to "background noise" status, but the reality is that when decisions to drill hinge on extremely subtle changes in waveform character ("when this front-loaded trough begins to show signs of splitting into a doublet, we've got porosity," etc.), one cannot afford to be confusing geology with lateral changes in the embedded wavelet. In this short article we describe, and provide a mathematical justification for, a very simple technique which can help detect lateral changes in wavelet phase. The method entails first identifying a regionally stable and geologically "isolated" seismic event, then computing the instantaneous phase at the peak of the instantaneous amplitude (i.e., envelope) of the associated seismic waveform. Under certain restrictive conditions described below, the instantaneous phase evaluated at the peak of the instantaneous amplitude can be a good estimate of the wavelet phase.

In the first part of our paper, we describe the technique. Then we provide a mathematical foundation by showing the equivalence between Fourier phase and instantaneous phase at the envelope peak for the special case of a constant-phase band-pass wavelet with a boxcar amplitude spectrum. Next, we show that when the analysis window contains two overlapping wavelets, the instantaneous phase and the Fourier phase of the wavelet do not always coincide. We use a simple numerical example to explore the magnitude of the error introduced by the technique under such circumstances.

Background. Interestingly, instantaneous phase isn't usually discussed in the context of "phase" in the usual sense of the word (i.e., in the sense of Fourier phase of some portion of the seismic signal). Instead, most literature seems to focus on the fact that the instantaneous phase tends to emphasize event continuity. However, there are at least two notable exceptions: Bodine (1984) showed an interesting result on synthetic data, namely that instantaneous phase evaluated at the envelope peak is equal to Fourier phase for a constant-phase trapezoidal-band-pass wavelet. Also, White (1991) exploited this intuitively-rooted property in an interesting paper illustrating a technique (which he credited to Turhan Taner) to estimate wavelet phase from a seismic trace via histogram analysis of instantaneous phase values measured at the envelope maxima.

Clearly this property that Fourier phase equals instantaneous phase at envelope peak for an isolated band-limited wavelet doesn't represent some new discovery. So why revisit it in the present paper? Well, aside from the fact that this property serves as the foundation for the aforementioned lateral wavelet stability tool, it seems to be somewhat overlooked by the seismic community at large (at least, according to our informal polling), so we hope to rekindle
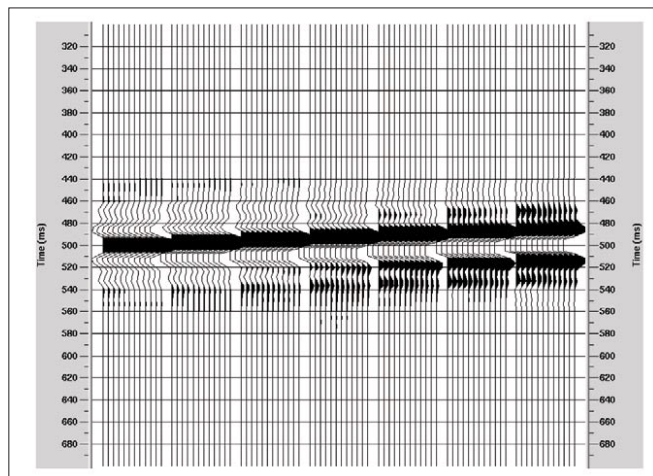
Figure 1. *Seven "trace bundles," each consisting of 12 identical zero-phase traces rotated in steps of 30°.*
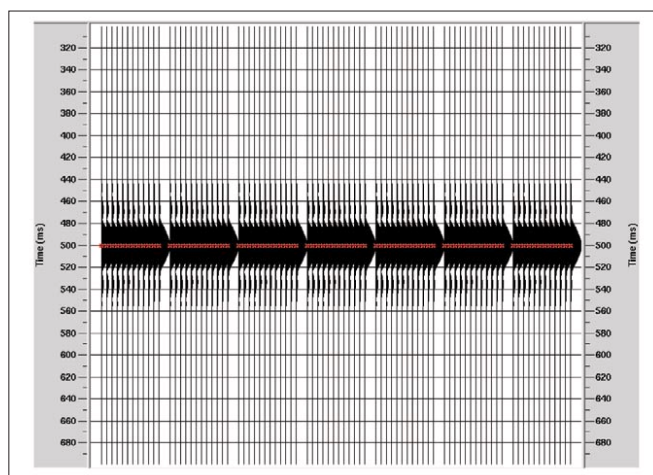
Figure 2. *Instantaneous amplitude of the zero-phase traces rotated in steps of 30°. Pick is on peak of amplitude envelope.*

awareness of its existence. Moreover, to our knowledge it has never been validated via formal mathematical proof (which we present below); rather, its existence seems to have been inferred from intuition and numerical experiments.

It's interesting to note that our following proof that instantaneous phase evaluated at envelope peak is equal to Fourier phase for a constant-phase boxcar/band-pass wavelet has a counterpart in the context of instantaneous frequency. Barnes (1991) proved that for any constant phase wavelet (this amounts to a somewhat broader class of wavelets than the boxcar/band-pass wavelets we are presently studying), the instantaneous frequency evaluated at the envelope peak is equal to the average Fourier spectral frequency weighted by its amplitude spectrum.
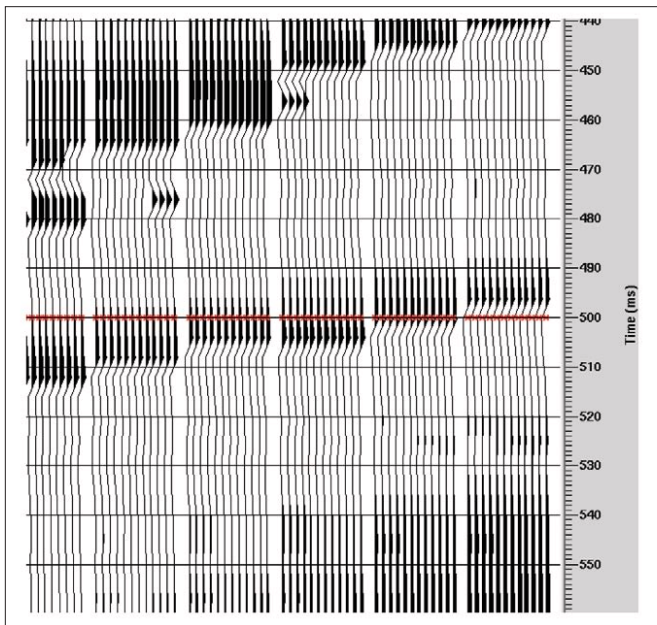
Figure 3. Instantaneous phase of the zero-phase traces rotated in steps of 30°, with pick on peak of amplitude envelope.
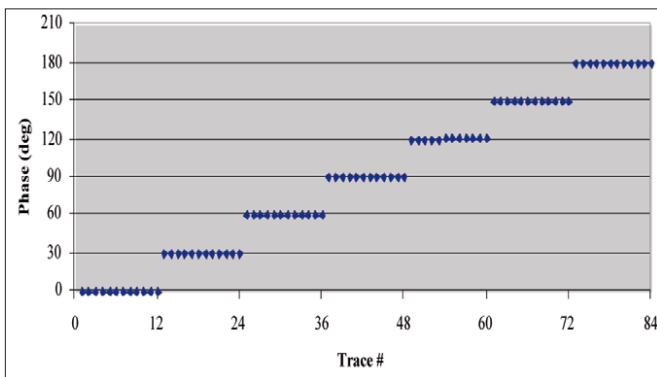
Figure 4. Instantaneous phase from Figure 3, extracted at the pick time (i.e., at the envelope peak).
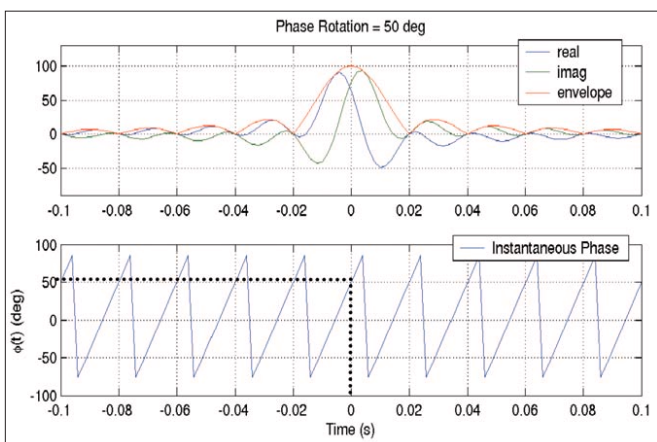
Figure 5. An analytic low-pass wavelet with constant phase rotation. The upper diagram displays the real and imaginary parts as well as the complex envelope. The lower diagram shows the instantaneous phase. Notice that the instantaneous phase at t = 0 (i.e., at the peak of the envelope) coincides with the true phase rotation.

We use a synthetic example to illustrate our methodology to compute phase variations along a seismic reflector. Figure 1 shows twelve band-pass wavelets rotated in steps of 30° from zero (no rotation) to 180°. Figures 2 and 3 show

the instantaneous amplitude (envelope) and instantaneous phase, respectively. Figure 4 displays the instantaneous phase measured at the peak of the envelope and we observe a perfect agreement with true phase of the wavelet. Thus, real-world implementation of the technique entails:

1) identification of a regionally stable, "isolated" seismic reflector;
2) computation of both instantaneous amplitude and phase along the reflector;
3) picking the peak of the instantaneous amplitude;
4) extracting (and displaying) the instantaneous phase at the pick time.

Technique limitations (read: disclaimer!) The technique's most attractive feature is that it's easy to use from the interpreter's viewpoint. This ease of use stems from the fact that many commercial interpretation packages allow ready computation of the requisite complex trace attributes, and of course by design they also offer good horizon pickers and easy result visualization. However, along with the technique's ease of use comes a rather limited realm of applicability (isn't that always the way of the world…). Specifically, the data must conform to a couple of rather restrictive assumptions.

First, the data set must contain an isolated, regionally stable seismic reflector. Although this might seem like a hopelessly restrictive requirement, it turns out that in many parts of the world such reflectors do exist—take for example, the reflection from the top of Wabamun Formation in many parts of the Western Canadian Sedimentary Basin. Still, violation of this assumption can lead to gross errors in wavelet phase estimation, as we'll see in a subsequent section where we apply the technique on a synthetic data set consisting of two overlapping wavelets (those who don't feel like wading through the ensuing math can fast track to Figure 6 to see this effect).

Second, the method assumes that the real-world embedded wavelet can be modeled as a constant-phase boxcar/band-pass wavelet. In reality, some wave propagation effects known to induce lateral variations in wavelet phase produce frequency-dependent phase and amplitude variations (e.g., the physical processes of stratigraphic filtering and anelastic attenuation), and such variations will not be properly modeled by the proposed technique.

Because of the above limitations, we are not touting the above technique as some sophisticated approach for deriving accurate measurements of wavelet phase; rather we see it as a "quick-and-dirty" red-flagging tool capable of identifying potential wavelet stability problems on many data sets. There are other more sophisticated lateral phase analysis techniques out there, including the popular technique of tracking lateral changes in phase rotation along several regionally stable, independent windows, and also mixed phase wavelet estimation via the use of third- or fourth-order statistics (e.g., Lazear, 1993).

Proof. We assume a constant-phase, band-pass wavelet where the amplitude spectrum is a boxcar function with upper and lower frequencies given by f_U and f_L, respectively, and corresponding upper and lower angular frequencies $B = 2\pi f_U$ and $b = 2\pi f_L$. The constant phase rotation is equal to c. The frequency domain expression for the analytic signal associated with this wavelet is obtained by doubling the Fourier components for non-negative frequencies, and zeroing them for negative frequencies. Thus, in the time domain we can write the analytic signal as:

Figure 6. (a) Synthetic seismogram composed of two wavelets separated by a delay τ. Both wavelets exhibit the same 50° constant-phase rotation; (b) envelope traces corresponding to (a); (c) instantaneous phase curves versus the delay τ. The red curve is the instantaneous phase evaluated at t=0 and the green curve is the instantaneous phase evaluated at the first envelope maximum (green curve "disappears" when red and green perfectly overlie one another). Note the ideal result is 50°; (d) same as (c), except the red curve is the instantaneous phase evaluated at $t = τ$ and the green curve is the instantaneous phase evaluated at the second envelope maximum. Note that when the wavelet separation is sufficiently large, the instantaneous phase at the peak of the envelope is a good estimate of the phase rotation.
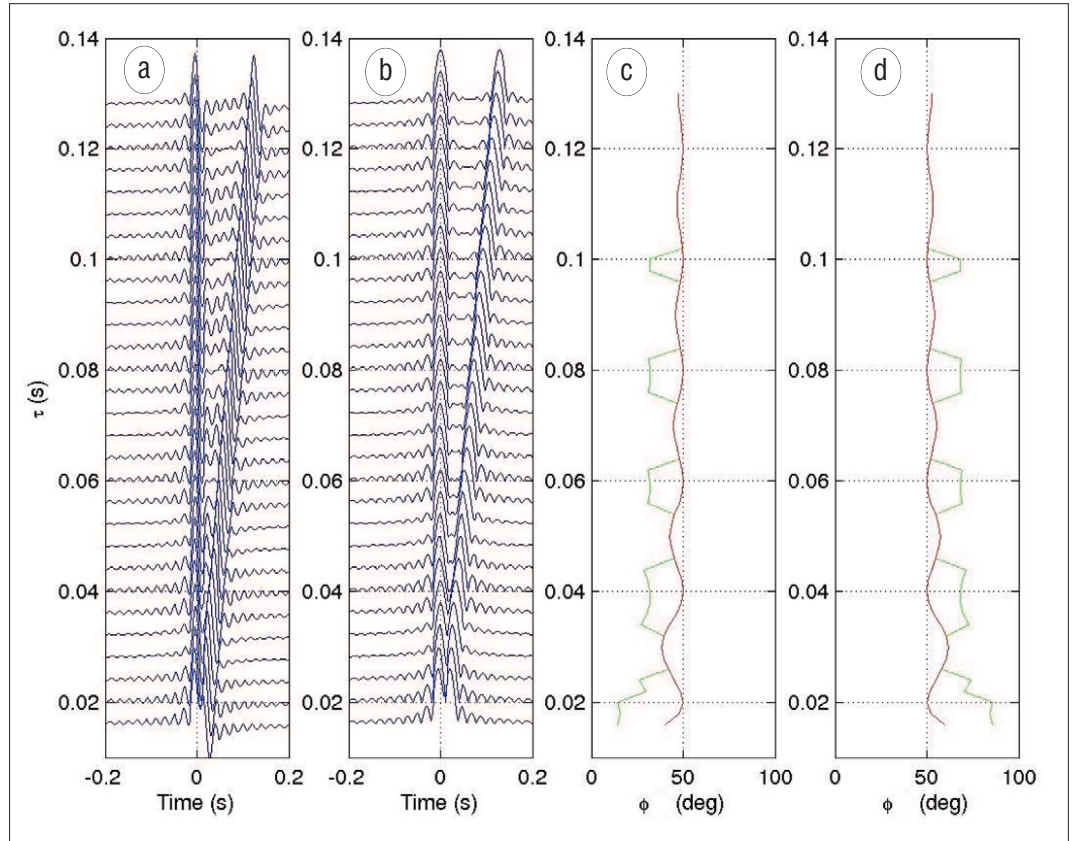
$$f_a(t) = \frac{1}{2\pi} \int_b^B 2e^{ic} e^{iwt} dw \qquad (1)$$

This complex analytic signal (Taner et al., 1979) can be written in terms of its real (the wavelet) and imaginary parts:

$$f_a(t) = R(t) + iG(t) \qquad (2)$$

After evaluating the integral in equation 1, we arrive at the following expressions:

$$R(t) = \frac{1}{\pi t}[sin(c+Bt) - sin(c+bt)] \qquad (3a)$$

$$G(t) = \frac{1}{\pi t}[cos(c+bt) - cos(c+Bt)] \qquad (3b)$$

The above expressions can be used to determine the instantaneous amplitude (envelope), $e(t)$, and the instantaneous phase, $\phi(t)$:

$$e(t) \equiv \sqrt{G(t)^2 + R(t)^2} = \frac{\sqrt{2[1 - cos((B-b)t)}}{\pi t} \qquad (4a)$$

$$tan[\phi(t)] \equiv \frac{G(t)}{R(t)} = \frac{cos(c+bt) - cos(c+Bt)}{sin(c+Bt) - sin(c+bt)} \qquad (4b)$$

It is interesting that the above expressions can also be used to rewrite the seismic wavelet in terms of a slow varying component, $e(t)$, and a time-dependent phase function, $\phi(t)$, as follows:

$$R(t) = e(t)cos[\phi(t)] \qquad (5)$$

where we have used the fact (from equation 4b) that

$$cos(\phi(t)) = R(t)/\sqrt{G(t)^2 + R(t)^2}$$

We see from equation 4a the well-known fact that the envelope does not depend on the phase rotation c. In other words, wavelets with different constant phase rotations will share the same envelope. It can also be shown that the envelope reaches its maximum at $t = 0$ with value

$$e(t = 0) = \frac{B - b}{\pi} \qquad (6)$$

We can use l'Hôpital's rule to evaluate the instantaneous phase at the maximum of the envelope:

$$\lim_{t \to 0} tan[\phi(t)] = \frac{sin(c)}{cos(c)} \qquad (7)$$

This last expression clearly shows that $\phi(t = 0) = c$. In other words, for the special case of an isolated band-pass wavelet characterized by a boxcar amplitude spectrum and a constant phase rotation, the instantaneous phase evaluated at the peak of the envelope function is equal to the constant phase rotation.

Figure 5 shows a single low-pass wavelet with phase rotation $c = 50°$ and maximum and minimum frequencies $f_U = 50$ Hz and $f_L = 0$ Hz, respectively. In the upper part of the diagram we display the real and imaginary parts of the analytic signal and also the associated envelope function. In the lower part we display the instantaneous phase. The instantaneous phase measured at the peak of the envelope

coincides with the true phase rotation of the wavelet, in harmony with our above mathematical analysis. It's interesting that the instantaneous phase is a periodic function (phase wraps as time progresses) with period given by $T = 2\pi / B = 1 / f_U$ (Figure 5, bottom). In our example the period is $T = 0.02$ s. This rapid variation in instantaneous phase with time has some negative implications for the robustness of the lateral phase analysis technique proposed in this paper, for it implies that the phase estimates will be very sensitive to errors in the envelope peak time. We'll explore this problem further in the following section.

Case of two overlapping wavelets. We will now analyze the error associated with estimating the phase rotation by using the instantaneous phase extracted at the peak of the envelope in the case of two partially overlapping wavelets. Specifically, we assume that the seismogram is composed of the superposition of two wavelets separated by an amount $t = \tau$, where the first wavelet is a scaled version of the second:

$$s(t) = R(t) + aR(t - \tau) \tag{8}$$

Because of the linearity of the Hilbert transform, it is easy to show that the analytic seismogram can be written as

$$s_a(t) = R(t) + aR(t - \tau) + i[G(t) + aG(t - \tau)]$$

and the corresponding instantaneous phase, ϕ_s, as

$$\tan[\phi_s(t)] = \frac{G(t) + aG(t - \tau)}{R(t) + aR(t - \tau)} \tag{9}$$

where the functional forms of $G(t)$ and $R(t)$ are given in equations 3a and 3b.

Now let's assume for the moment that the wavelet superposition effect does not "confuse" the picking of the envelope peaks. In other words, let's assume the envelope function contains two maxima, one at $t = 0$ and the other at $t = \tau$. We'll explore the validity of this assumption shortly. In this idealized case we would designate $\phi_s(0)$ to be the phase rotation estimated from the first wavelet and $\phi_s(\tau)$ to be the phase rotation estimated from the second wavelet. Then from equation 9 it is clear that the instantaneous phase evaluated at the peak of the envelope of the first wavelet is a good approximation to the true phase rotation, c, if and only if the contributions from the real and imaginary part of the second wavelet are negligible. Specifically, if $G(t-\tau)$, $R(t-\tau)$ have decayed sufficiently in the neighborhood of $t = 0$, then

$$tan[\phi_s(t = 0)] = \frac{G(0) + aG(-\tau)}{R(0) + aR(-\tau)} \approx \frac{G(0)}{R(0)} \tag{10}$$

and from the first equality in equation 4b, it follows that

$$tan(\phi_s(t = 0)) \approx tan(\phi(t = 0)) \tag{11}$$

and from equation 7, we see that $\phi_s(t = 0) \approx c$. The same analysis is valid for the instantaneous phase extracted at $t = \tau$. Thus it is clear that when τ is large enough, the two estimates, $\phi_s(0)$ and $\phi_s(\tau)$, will coincide with the true phase rotation of the wavelet.

Figure 6a shows the proposed seismogram model for variable τ and $a = 1$, where both of the wavelets are identical in shape to the single wavelet we analyzed in the pre-vious section. The associated envelope traces are shown in Figure 6b. We have extracted the instantaneous phase at $t = 0$ and $t = \tau$ (red curves in Figures 6c and 6d, respectively), corresponding to this idealized situation where the envelope peaks are not distorted due to sidelobe interference effects associated with the tuning of the two wavelets. Note that the error in the phase estimate is acceptably small for all the τ values we investigated, reaching a maximum value of approximately $\pm 15°$ at $t = 0.02$ s (we arrived at this happy conclusion based on the interpreter's rule of thumb that says that phase rotations up to $30°$ don't typically impact the visual appearance of stratigraphic character plays). Also note that the error diminishes asymptotically as τ grows, and that the instantaneous phase exhibits an oscillatory behaviour (when plotted as a function of τ), owing to the sinusoidal nature of both the real and imaginary parts in equation 10.

Of course in reality, the envelope maxima will not necessarily occur at $t = 0$ and $t = \tau$ if the wavelets are sufficiently close together. To what degree does this effect hinder our analysis? In an effort to investigate this question, we portray the more realistic situation in which the instantaneous phase is extracted at the first and second envelope maxima (green curves in Figures 6c and 6d, respectively), rather than at $t = 0$ and $t = \tau$. Now the error in the phase estimate is significantly worse, with acceptable phase estimates being obtained only for values of τ greater than 0.1 s (it must be noted that for $\tau < 0.1$ s, there do exist piecewise continuous regions in τ where the error is small—more about this strange pattern later—but these regions are proximal to regions in which the error is large, so one must conclude that for practical purposes the error is large for $\tau < 0.1$ s). Clearly, the technique suffers from the cascading of two errors; one due to the interplay between sidelobe interference and the location of the envelope peaks, and the other due to the interplay between sidelobe interference and the instantaneous phase attribute itself. In the case of this specific synthetic test, the majority of the error is due to the envelope peak "mispositioning" effect.

The fact that the error associated with the mispositioning effect is large is consistent with our observation for the single wavelet study that the time derivative of the instantaneous phase is large (Figure 5, bottom). From this figure, it's clear that a change in $\dot{\phi}(t)$ of merely 0.002 ms (one sample) implies a $20°$ change in the instantaneous phase. This helps to explain the "sparse sawtooth" appearance of the green curves in Figures 6c and 6d. The "teeth" correspond to regions where the envelope peak deviates from $t = 0$ (or $t=\tau$) by merely one sample.

Finally, it's important to note that our quantitative inferences about reliable phase estimates as a function of wavelet separation are drawn from the specialized case of two noise-free overlapping equal-amplitude, constant-phase, boxcar/band-pass wavelets. In the real world, the best we can do is to qualitatively caution against using this technique on noisy data, or in cases where the analysis horizon shows contamination by events which "fade in and out" of the analysis window as a function of lateral position.

Conclusions. We provide a mathematical proof of a known property (which to date appears to have been inferred from numerical experiments), namely that the instantaneous phase evaluated at the envelope peak is equal to the Fourier phase in the case of a constant-phase, band-pass wavelet with a boxcar amplitude spectrum. We also describe a simple lateral wavelet stability analysis tool which exploits this property. The tool is capable of producing reliable estimates

of wavelet phase if the data set contains a reasonably noise-free, regionally stable, lithologically isolated event, and moreover, if the wavelet can be accurately modeled via a constant-phase boxcar/band-pass wavelet. In the case where more than one reflector encroaches on the analysis window, the technique will produce erroneous results. T|E

Suggested reading. "Instantaneous frequency and amplitude at the envelope peak of a constant-phase wavelet" by Barnes, (GEOPHYSICS, 1991). "Waveform analysis with seismic attributes" by Bodine (*SEG 1984 Expanded Abstracts*). "Mixed-phase wavelet estimation using fourth order cumulants" by Lazear (GEOPHYSICS, 1993). "Complex seismic trace analysis" by Taner et al. (GEOPHYSICS, 1979). "Seismic attributes revisited" by Taner et al. (*SEG 1994 Expanded Abstracts*). "Properties of instantaneous attributes" by White (THE LEADING EDGE, 1991). *Seismic Data Analysis: Processing, Inversion, and Interpretation of Seismic Data* by Yilmaz (SEG, 2001).

Corresponding author: perzm@geo-x.com